Review

Red Mud as a Secondary Resource of Low-Grade Iron: A Global Perspective

Rita Khanna [1,*], Yuri Konyukhov [2], Dmitry Zinoveev [3], Kalidoss Jayasankar [4], Igor Burmistrov [5], Maksim Kravchenko [6] and Partha S. Mukherjee [7]

[1] School of Materials Science and Engineering (Ret.), The University of New South Wales, Sydney, NSW 2052, Australia

[2] Department of Functional Nanosystems and High-Temperature Materials, National University of Science and Technology "MISiS", 119049 Moscow, Russia; ykonukhov@misis.ru

[3] A.A. Baikov Institute of Metallurgy and Materials Science, Russian Academy of Science, 119334 Moscow, Russia; dzinoveev@imet.ac.ru

[4] Materials Science & Technology Division, CSIR-National Institute for Interdisciplinary Science and Technology, Thiruvananthapuram 695019, India; jayasankar.met@gmail.com

[5] Engineering Centre, Plekhanov Russian University of Economics, 117997 Moscow, Russia; burmistov.in@rea.ru

[6] Moscow Power Engineering Institute, National Research University, 111250 Moscow, Russia; Kravchenkomv@mpei.ru

[7] Institute of Minerals and Materials Technology (Ret.), Council of Scientific and Industrial Research, Bhubaneshwar 751013, India; psmukherjee52@gmail.com

* Correspondence: rita.khanna66@gmail.com; Tel.: +61-043415-5956

Abstract: Managing red mud (RM), a solid waste byproduct of the alumina recovery process, is a serious ecological and environmental issue. With ~150 million tons/year of RM being generated globally, nearly 4.6 billion tons of RM are presently stored in vast waste reserves. RM can be a valuable resource of metals, minor elements, and rare earth elements. The suitability of RM as a low-grade iron resource was assessed in this study. The utilization of RM as a material resource in several commercial, industrial operations was briefly reviewed. Key features of iron recovery techniques, such as magnetic separation, carbothermal reduction, smelting reduction, acid leaching, and hydrothermal techniques were presented. RMs from different parts of the globe including India, China, Greece, Italy, France, and Russia were examined for their iron recovery potential. Data on RM composition, iron recovery, techniques, and yields was presented. The composition range of RMs examined were: Fe_2O_3: 28.3–63.2 wt.%; Al_2O_3: 6.9–26.53 wt.%; SiO_2: 2.3–22.0 wt.%; Na_2O: 0.27–13.44 wt.%; CaO: 0.26–23.8 wt.%; Al_2O_3/SiO_2: 0.3–4.6. Even with a high alumina content and high Al_2O_3/SiO_2 ratios, it was possible to recover iron in all cases, showing the significant potential of RM as a secondary resource of low-grade iron.

Keywords: red mud; iron recovery; waste utilization; smelting; low grade iron ore; reduction

1. Introduction

Bauxite, recognized as the key aluminum ore, contains ~30–54% alumina (Al_2O_3) along with mixtures of silica, iron oxides, titanium dioxide, and several impurities, etc. Up to 95% Al is produced worldwide from the bauxite ore using the Bayer's process. In the Bayer process, bauxite is washed in a hot solution of sodium hydroxide, which leaches Al in the form of $Al(OH)_3$; it is later calcined to form Al_2O_3. Red mud (RM), also known as the bauxite residue, is a solid waste byproduct of the alumina recovery process. Producing one ton of alumina consumes up to 2–3 tons of bauxite and generates ~0.4–2 tons of RM depending on the source/location of the ore; the global average of RM is ~1.3 tons per ton of alumina [1,2]. Alumina has also been extracted from poor-quality diasporic bauxite using soda lime sintering at high temperatures [3]. Wang and Liu (2012) [4] have reported

on the chemical composition of Bayer and sintering red muds from an alumina refining plant in Guizhou, China [4]. While the typical composition of Bayer RM was Fe_2O_3 (26.4%), Al_2O_3 (18.9%), SiO_2 (8.52%), CaO (21.8%), and TiO_2 (7.4%), the corresponding results for the sintering RM were Fe_2O_3 (7.9%), Al_2O_3 (17.3%), SiO_2 (17.3%), CaO (40.2%), and TiO_2 (7.4%). The sintering RM showed much higher levels of CaO and SiO_2 but low levels of Fe_2O_3 as compared to the Bayer RM; similar trends have also been reported by Feng and Yang (2018) [5]. Due to quite low levels of Fe_2O_3 present, sintering RM is not considered a potential iron resource in this study.

Global bauxite resources are estimated to be ~55 to 75 billion tons with reserves in Africa (32%), Oceania (23%), South America, the Caribbean (21%), and Asia (18%). With the annual primary aluminum production increasing to 47 million tons, an estimated 150 million tons of RM are being produced in various aluminum plants across the world [6,7]. Nearly 4.6 billion tons of RM, presently stored around in vast waste reserves, represents massive industrial waste scenarios [8–10]. Several red mud incidents in different countries have also been tabulated in a number of publications [11,12].

Extensive efforts and attempts have been made to recycle, process, and utilize RM waste. Several excellent reviews are available in the literature on RM recycling, utilization, and management [13–20]. Key challenges in processing RM include, among others, high alkalinity pH: 10–13 [21], high moisture content, small particle sizes (≤75 μm), large volumes, and transportation costs [22]. Landfilling and dumping around the industrial plants have been the standard procedure; vast quantities of stockpiled RM are known to be toxic and very hazardous [23]. Deep sea dumping and storage in ponds have also been attempted. Poorly designed storage dams are likely to fail under certain circumstances resulting in local and environmental contamination [24]. Numerous efforts are being made to find economically viable and environmentally sustainable solutions to the RM problem. However, most current options can only accommodate a small fraction of the red mud generated globally [25,26].

Depending on the region and the location, the type of bauxite, operating parameters of the Bayer process, and the composition of red mud can vary over a wide range [27]. Major constituents of RM are: Fe_2O_3: 26.6–46 wt.%; Al_2O_3: 15–21.2 wt.%; TiO_2: 4.9–21.2 wt.%; SiO_2: 4.4–18.8 wt.%; Na_2O: 1–10.3 wt.%; CaO: 1–22.2 wt.% [28,29]. Several minor elements (U, Ga, V, Zr, Sc, Cr, Mn, Y, Ni, Zn, Th, rare earths) may also be present in ppm levels [30]. RM particles are generally fine-grained with particle sizes smaller than 75 μm for up to 90 wt.% of particles, and surface areas ranging between 10–30 m^2/g [31]. Given the complex composition of RM, fine particle sizes and toxic caustic-corrosive nature, the processing of RM can be quite challenging, and technically difficult [32].

Global steel production has more than tripled over the past 50 years; China and India are the top two steel producing nations. In 2020, the global steel production was 1.86 billion tons; China accounted for more than a billion tons of steel [33]. Iron ore resources are getting consumed at a fast rate leading to a reduced availability of high-grade iron ores as well as sharp declines in their supply to iron and steel plants. The current scenario is steadily shifting towards the use of low grade iron ores. Presently, red mud is not considered as competitive raw material for iron and steel making as the Fe_2O_3 content of the red mud (27–47%) is significantly lower than the requisite concentrations in conventional iron ores (>60%) [34]. Iron ores with Fe contents above 65% are regarded as high-grade ores; 62–64% medium grade ores and those below 58% Fe are considered as low-grade ores [35,36]. The known world resources of crude iron ores are approximately 800 billion tons [37]. Most of the known deposits contain low-grade ores with iron contents even less than 30%. In order to meet the growing demand for iron and steel, it is thus imperative to find new sources of iron ore to supplement the existing reserves [38].

With significant reserves of iron, albeit in relatively low concentrations, the RM waste could be considered as a low-grade iron ore. However, requisite high volumes, fine particle sizes, high moisture, and alkaline content make it virtually impossible and too costly to transport large quantities of RM to distant places. Commercial scale iron recovery, therefore,

needs to be carried out near the source of RM generation. Across the globe, there are wide variations in RM compositions as well as methodologies used to recover iron.

The aim of this study is to develop a critical review and an assessment on the recovery of iron from RMs in different parts of globe. This study will consolidate relevant data from India, China, Greece, Italy, France, and Russia in the form of case studies to determine the likelihood of iron recovery processes, tailored to local conditions and RM compositions. The article is organized as follows. A brief overview on RM waste management strategies is presented in Section 2. Section 3 presents key techniques used for the recovery of iron from red mud. Consolidated results from the global scenario are presented in Section 4 in the form of case studies. These discussions are followed by a comparison of RMs with low grade iron ores and concluding remarks in Sections 5 and 6.

2. RM Waste Management Strategies: A Brief Overview

A brief overview of RM waste management practices is presented next with specific focus on recycling, utilization, and material recovery. Attempts have been made to recycle large volumes of RM in several commercial, industrial operations such as building and construction materials, cement, concrete, coloring agents for paints, paper/polymer/ceramic/refractory products, catalysts, inorganic chemicals, adsorbents, metallurgical recovery of metals (Al, Ti, Si), rare earth elements, and others [39,40]. Being the focus of this study, specific details on the recovery of iron from red mud will be presented in later sections. Some of the key approaches to RM utilization are summarized below.

2.1. Construction Materials

2.1.1. Cement

The use of RM in the production of cement has been investigated extensively in several countries. Road construction using RM is considered one of the most suitable applications [41]. High contents of iron and aluminum in RM were reported to be beneficial for cement production, accelerating the clinkering process and for slag replacement. Pontikes and Angelopoulos [42] have recommended the addition of ~30 kg of RM per ton of ordinary Portland cement. Feng et al. [43] mixed 50 wt.% thermally active RM with modifiers along with other solid wastes to produce Portland cement; the flexural and compressive strength of the manufactured concrete were found to be adequate for concrete requirements of pavement materials. Liu and Poon [44] used RM to prepare self-compacting concrete; Nikbin et al. [45] evaluated the mechanical strength, elastic moduli and environmental impact of lightweight concrete. RM from HINDALCO (Hindustan Aluminum Corporation, Mumbai, India) has been used to prepare superior strength Portland cements; typical compositions used were: 30–35% RM, 15–20% bauxite, 7.5–10% gypsum, 45–50% lime [46]. The crushing and bending strength of the mortar were found to improve with 5–10% RM addition [47].

2.1.2. Building Materials

Dodoo-Arhin et al. [48] investigated composites of RM (20–50 wt.%) and Tetegbu clay (balance) for making ceramic bricks. Sintered bricks were fired in the temperature range 800–1100 °C; optimal properties for the construction brick applications were obtained for RM contents of 50 wt.%. Several researchers [49–54] have examined the potential recycling of RM for construction and building supplies, different types of bricks such as non-fired, non-steam cured bricks, ceramic glazed tiles, decorative bricks, hollow bricks, fly ash bricks, and others; their strength and quality was found to be quite comparable to standard bricks. Stabilized blocks with strength of grades II/III bricks have been developed mixing RM with clay and/or fly ash; low density (1.1–1.2 g/cm^3), hollow bricks and blocks have also been prepared [55,56].

2.1.3. Glass-Ceramics, Geopolymers, Catalysts

Some other applications of RM include utilization in the production of glass-ceramics, geopolymers, catalysts, and fillers, among others. Firing blends of RM with limestone

at 1150 to 1200 °C, Amritphale et al. [57] were successful in producing cements with a strength of 200 kg/cm^2. Ceramic tiles were also produced from mixtures of RM with fly ash/additives; relative proportions of various constituents were used for controlling the tile strength [58,59]; RM has also been used to reduce the impact of glazing [60]. Yang et al. [61] were able to prepare a CaO-SiO$_2$-Al$_2$O$_3$ glass-ceramics using up to 85% waste materials (RM and fly ash). The limitations of RM in terms of colour and impact strength and densification mechanism could limit some commercial applications [62].

Geopolymers and synthetic aluminosilicates have been produced from mixtures of RM with fly ash other wastes such as FeNi slag, rice husk ash, blast furnace slag, etc. as a replacement for Portland cement ceramic and composite applications [63,64]. Advanced composites are used extensively in defence, aerospace, petrochemical, and marine industries [65]. Using RM as base and filler materials, a 4 km long highway was trialed in Zibo, Shandong Province, China and was found to meet requisite strength requirements [66]. RM has been used as a catalyst in several applications, e.g., hydro-dechlorination, coal hydrogenation, coal/biomass liquefaction, SO$_2$ reduction, methane combustion etc. [67,68]; However, only a small fraction of RM waste can be used in these applications. Environmental pollution control applications of RM include waste water treatment, soil remediation with bauxite residues, waste gas purification and sulphur removal, etc. [69–71].

2.2. Resource Recovery of Metals

Depending on the region & the location, the type of bauxite, operating parameters of the Bayer process, the composition of red mud can vary over a wide range [72]. Major constituents of RM are: Fe$_2$O$_3$ Al$_2$O$_3$, TiO$_2$, SiO$_2$, Na$_2$O, CaO etc. [73–76]. Several minor elements (U, Ga, V, Zr, Sc, Cr, Mn, Y, Ni, Zn, Th, rare earths) may also be present in ppm levels [77–79]. RM particles are generally fine-grained with particle sizes smaller than 75 μm for up to 90 wt.% of particles, and surface areas ranging between 10–30 m^2/g. Given the complex composition of RM, fine particle sizes, high moisture content and toxic caustic-corrosive nature, the processing of RM can be quite challenging and technically difficult [32,80]. Some of the techniques used to extract key metals from RM are briefly summarized below.

2.2.1. Aluminium

Up to 4–16% aluminum could be present in RM after Bayer's process as residual alumina; several hydro/bio metallurgical approaches have been developed for processing RM as an additional alumina resource. Vachon et al. [81] used mixtures of sulphuric/citrus/oxalic acids in a range of proportions for extracting aluminum from RM. These authors also investigated bioleaching using acid-producing bacteria and fungi recovering up to 75% Al present. Bruckard et al. [82] used fluxing, smelting and leaching at 60 °C with soda and calcium carbonate to dissolve up to 55% Al. The hydrometallurgical approach involves atmospheric/pressurized alkali leaching at high temperatures as well as acid leaching. Zhang et al. [83,84] were able to recover alumina by forming andradite–grossular hydrogarnet in a hydrothermal process. The pyrometallurgical recovery involves sintering with soda (25–70 wt.%) and lime (10–50 wt.%) in the temperature range 1000–1050 °C to form water-soluble sodium aluminate, followed by leaching in water/NaOH (1.5–2 M) achieving up to 76–90% aluminum extraction [85,86]. However, some of these processing methods could be quite expensive, time consuming and produce secondary waste products as well.

2.2.2. Titanium

Pyrometallurgical as well as hydrometallurgical techniques have been used for extracting TiO$_2$ from RM. Calcining RM in the temperature range 850–1300 °C, followed by smelting with a carbonaceous reductant in an electric furnace, produces molten iron along with a slag containing titanium dioxide, alumina, silica, etc. [87–89]. Kasliwal and Sai [90] leached RM with HCl at 363 K, and heat treated the leach residue with Na$_2$CO$_3$ at 1423 K

for 115 min to recover up to 76% TiO_2. Deep et al. [91] used hydrolysis and calcination followed by acid leaching with (3% H_2O_2, 0.5 M H_2SO_4, 4 M HCl/H_2SO_4) solution to recover TiO_2. The commercialization of these predominantly laboratory based techniques would require significant resources and associated infrastructure.

2.2.3. Rare Earths and Other Elements

RM also contains several rare earth elements (REEs), including scandium (60–120 ppm), yttrium (60–150 ppm), gallium (60–80 ppm), as well as radioactive elements uranium (50–60 ppm) and thorium (20–30 ppm) [92–97]; some of these concentrations are comparable or even better than corresponding concentrations in respective ores. REEs are generally recovered from RM using the hydrometallurgical route. Wang et al. [98] recovered scandium from synthetic RM using solvent extraction with Di-(2-ethylhexyl) phosphoric acid. Through selective leaching of a Greek RM with dilute HNO_3, Ochsenkuhn-Petropulu et al. [99] were able to recover up to 90% Y, ~70% heavy lanthanides (Yb, Dy, Er), ~50% middle lanthanides (Nd, Sm, Eu, Gd) and 30% light lanthanides (La, Ce, Pr). Mineral as well as organic acids were used by Ujaczki et al. [100] to leach out REEs from the RM. Selective recovery of up to 75% Sc can be achieved from RM by using the sulfation method [101]

3. Iron Recovery from Red Mud: Key Techniques

Iron is one of the key constituents of RM and is often present as oxides or oxyhydroxides. Several techniques such as magnetic separation, carbothermal reduction, microwave carbothermal reduction, smelting reduction, acid leaching, and hydrothermal techniques have been developed to separate and recover iron-bearing phases [102,103]. A brief summary of the methods used is presented below.

3.1. Magnetic Separation

The main mineral phase of iron in RM tailings could be hematite, goethite, or magnetite, which are magnetic or weakly magnetic materials. One of the most effective ways to separate the fine magnetic particles in liquid suspensions is through direct application of high intensity magnetic fields; electromagnets with fields up to 0.3 T (Tesla) have been used for recovering Fe from RM slurry. The yield was generally quite poor with the resulting output in the form of magnetic and non-magnetic fractions [104]. A direct magnetic separation approach is inefficient for Fe recovery from RM due to the lack of magnetic iron-bearing mineralogical phases. Much stronger fields (up to 4 T) using superconducting magnets have also been used to separate the fine magnetic particles (<100 μm) in liquid suspensions and to separate iron rich and iron poor fractions [105]. After the separation process, high iron content and low iron content parts of RM could be recycled as resources in different industrial sectors. Higher magnetic intensity leads to more amounts of concentrates being collected and higher iron contents in the concentrates. Using hydro cyclone and magnetic separation techniques, it was possible to raise the iron content of RM from 52 wt.% to 70 wt.% [106].

3.2. Carbothermal Reduction

The carbothermal reduction of red mud has been reported using several techniques such as smelting [107], microwave reduction [108], suspension roasting [109], and sintering [110]. In the carbothermal reduction, RM powders are mixed with a range of carbonaceous materials (coals, coke, charcoal, graphite, bagasse, spent pot lining etc. [111,112] and sodium flux to produce pellets/briquets followed by heat treatment in the temperature range between 600–1200 °C for time periods between 30–240 min. This technique is limited by the low grade of iron produced, economic costs of the flux and reductants used, and high energy consumption.

3.3. Microwave Carbothermal Reduction

This technique uses isothermal/non-isothermal reduction using microwave heating followed by magnetic separation [113,114]. Microwave heating has several advantages over conventional heating, such as the instantaneous generation of heat inside moderately absorptive materials rather than relatively slow heat transfer from the outside surface. Typical processing conditions are 600–1000 W power, 700–1000 °C temperature range, 5–20 min roasting time and 5–16 wt.% C. Reductants used include charcoal and CO/CO_2 gases. Microwave heat treatment is followed by low intensity (0.1–1.8 T) magnetic separation. This treatment has significantly faster reaction times and potentially lower energy consumption as compared to conventional heat treatment methods [115]. Some of the limitations of this technique include high costs of reductants, low grade iron recovery and scaling issues.

3.4. Smelting Reduction

Smelting reduction involves the roasting of red mud, reductant and flux pellets in the temperature range 1400–1750 °C for times between 15 to 60 min. Furnaces used include resistance furnace, electric arc furnace, plasma furnace, vertical tube furnace, etc. [116–123]. Coal, coke, graphite, blast furnace sludge, and biomass have been used as reductants [124]. Additives during pellet making include Na_2CO_3, $CaCO_3$, Na_2SO_4-Na_2CO_3, among others. Under the ENEXAL project, Balomenos et al. [125] have reported on the reductive smelting of red mud and coke in electric arc furnace based experiments, preliminary thermodynamic modelling, and transition to full-scale pilot plant operation. Typical post treatments included the separation of metal and slag and acid leaching; end products were in the form of pig iron, iron nuggets, and REE enriched solutions. While high grade iron (91–96%) could be recovered, the limitations of this technique include high energy and flux consumption, high levels of phosphorus, and sulphur in iron and generally low yields.

3.5. Suspension Reduction

In this technique, RM undergoes reduction with reducing gases CO, CO_2, and H_2 combined with N_2 in a fluidized/static bed reactors [126–128]. This technique offers an alternate processing route for the separation of iron bearing phases from RM and the residue valorization via hydrogen reduction followed by magnetic separation. Typical temperature ranges and heating times were 350–600 °C for 30 min and 500–640 °C for 15–30 min. Key advantages of this method are relatively low processing temperatures, low energy consumption, no need for sintering or agglomerating the residue, and negligible carbon contamination typically observed in carbothermal reduction. This method is, however, limited by the high cost of H_2, poor iron enrichment, complex design, and composition variables.

3.6. Hydrometallurgy

A number of hydrometallurgical processes based on acid leaching have been developed for extracting iron from red mud. The metallic values in red mud are leached using mineral acids: HCl, H_2SO_4, HNO_3, H_3PO_4, and organic oxalic acid followed by solvent extraction [129]. An extraction rate of 96% could be achieved after leaching with 1 mol/L oxalic acid at 75 °C for 2 h. UV radiation was used on the precipitates for transforming ferric oxalate to ferrous oxalate [130]. Leaching with 8 N sulphuric acid at 100 °C for 24 h, an iron recovery of 47 wt.% could be achieved [131]. Iron grade recovery ranged from 94.2–97.4 wt.% for oxalic acid, 52–95.9 wt.% for hydrochloric acid, and 40–97.4 wt.% for sulphuric acid [132,133]. However, this technique is uneconomical for large scale utilization and nonselective iron extraction, and suffers from secondary waste generation and requires further downstream processing.

3.7. Other Techniques

Being ecological and requiring low energy consumption, bio-metallurgical techniques based on bioleaching are becoming increasingly important for the treatment of iron oxide ores [134,135]. Desulfuromonas palmitatis is believed to dissolve part of iron minerals from bauxite; especially 95% of amorphous ferrihydrite can be dissolved. The high pH value of red mud is likely to restrict the use of bioleaching for extracting of iron oxides [136]. Vakilchap et al. [137] observed that Aspergillus niger fungus can recover up to 69.8% Al, 60% Ti, and 25.4% Fe from red mud; a holding time of 30 days was required. Penicillium tricolor fungus has also been used for REE recovery from red mud [138,139]. In the hydrothermal method, red mud is digested in an alkaline medium at high temperatures (40% NaOH, 250 °C, 30–180 min), followed by washing and magnetic separation. [140]. Iron values present in red mud can be extracted using both the pyrometallurgical and hydrometallurgical techniques. Oxalic acid leaching, coupled with photocatalytic reduction, may be suitable for low iron grade red mud. Carbothermal microwave reduction followed by magnetic separation presents a high efficiency technique for red muds with 25–40% iron values. The choice of recovery technique will be based on economic feasibility, efficiency, as well as recovery efficiency.

4. Global Scenario

In this section, we present an overview on red muds being used a secondary iron resource in different countries around the globe. Details will be provided on the composition of red mud, iron recovery technique used, product yield and other relevant features in the form of case studies. As high temperature processing and pyrometallurgy are traditional approaches in conventional ironmaking, in this section we have focused our specific attention on the pyrometallurgical recovery of iron from red muds using well-established techniques.

4.1. INDIA

4.1.1. Case Study 1

In this study, the red mud was sourced from HINDALCO India and the Bauxite type was Laterite [113]. The chemical composition of RM is given in Table 1.

Table 1. Chemical composition of red mud [113].

Constituent	Fe_2O_3	Al_2O_3	SiO_2	TiO_2	CaO	Na_2O	Iron Grade
wt.%	36.26	16.58	8.32	17.10	1.43	6.00	25.7%

As received RM powder was pulverized using a ball mill to sizes below 100 μm and concentrated to an iron rich fraction using magnetic separation, followed by reduction roasting pre-treatment. Reduction investigations were carried out in the temperature range (700–1000 °C) using a silica crucible in a standard muffle furnace as well as in a 900 W microwave furnace. Charcoal was used as the reductant in both furnaces and the heating times were between 10–50 min. A coating of calcium oxide was used from trapping CO_2 gas over period of time. Specimens were water quenched after the heat treatments. Magnetic separation was carried out on reduced samples using 0.2 T magnetic field. Heat treatment temperature and heating time were found to be key factors in iron recovery. A treatment at 1000 °C for 10 min resulted in 95% iron recovery and an increase in RM iron content to 48.5 wt.%.

4.1.2. Case Study 2

In this study, the red mud was sourced from NALCO India; Bauxite type used was Laterite [114]. The chemical composition of RM is given in Table 2.

Experimental steps used in this study were quite similar to those in Case Study 1 and involved the blending of red mud with charcoal reductant, carbothermal reduction in muffle, and microwave furnaces followed by magnetic separation. Optimal experimental conditions for iron grade and iron recovery were determined. In the muffle furnace, optimal

conditions for iron grade and iron recovery were 1000 °C, 16.5 wt.% C, 50 min and 850 °C, 11 wt.% C, 50 min, respectively. Corresponding conditions for the microwave furnace were 1000 °C, 11 wt.% C, 10 min and 850 °C, 5.5 wt.% C, 30 min, respectively.

Table 2. Chemical composition of red mud [114].

Constituent	Fe_2O_3	Al_2O_3	SiO_2	TiO_2	CaO	Na_2O	Iron Grade
wt.%	47.85	22.64	10.25	3.58	1.86	10.25	33.5%

4.1.3. Case Study 3

Jayasankar et al. [117] used thermal plasma technology to produce pig iron from RM, as well as from low grade iron ore fines. The RM was sourced from NALCO India; its composition is provided in Table 3. The term LOI represents 'loss on ignition'.

Table 3. Chemical composition of red mud [117].

Constituent	Fe_2O_3	Al_2O_3	SiO_2	TiO_2	CaO	Na_2O	LOI
wt.%	49.65	6.86	22.0	-	-	8.29	11.39%

The plasma furnace used in this study uses a pot type 35 kW DC extended transfer arc plasma reactor; zircon coated graphite crucibles were used as the furnace hearth [141]. Size reduced powders were placed in the graphite crucible of the plasma reactor. 1 kg of RM was mixed with 30% petroleum coke and 10% dolomite; the presence of dolomite helped in the separation of Fe from the slag. Graphite was also used as a reductant in some cases. These blends were loaded in the crucible. The plasma furnace was operated using 250 A current and a DC voltage of 60 V. Argon gas was passed continuously through the furnace at a flow rate of 1 L/min. Blends were smelted in the temperature range 1550–1650 °C for times between 20–30 min. The smelted pig iron and slag were collected into a preheated graphite mould through a tap hole. Iron recovery of 78% and 48% was achieved for graphite and petroleum coke reductants.

4.2. CHINA

4.2.1. Case Study 4

Li et al. [142] collected red mud from Shandong Province, China; the sample was pre-dried at 100 °C for 10 h to remove moisture. The chemical composition is given in Table 4.

Table 4. Chemical composition of red mud [142].

Constituent	Fe_2O_3	Al_2O_3	SiO_2	TiO_2	CaO	Na_2O	LOI
wt.%	47.76	10.26	2.25	4.22	0.26	1.13	11.93%

The RM, flux, and bentonite binder were mixed thoroughly to prepare green balls (800 mm dia., 200 mm thickness) in a disk pelletizer; these were later dried using a vacuum oven. Bituminous coals were used reductants and mixed with dry pellets with C/Fe mass ratio of 1.5. These were heat treated in a muffle furnace at 1050 °C for 80 min and furnace cooled. About 50 gm of pre-reduced pellets were mixed with 10% C and smelted at 1600 °C for 30 min; a corundum crucible was used during smelting. Pig iron and slag were cooled to room temperature under N_2 atmosphere for subsequent separation. The pig iron was produced with an iron recovery of 98.15% and the slag containing 43.17% Al_2O_3 and 15.71% TiO_2, respectively.

4.2.2. Case Study 5

Chun et al. [143] investigated the recovery of iron from red mud using high temperature reduction of carbon bearing RM briquettes. The red mud was collected from Shandong

Aluminum Corporation, China. Up to 80% particles could pass through a 0.1 mm sieve. The composition of red mud is given in Table 5.

Table 5. Chemical composition of red mud [143].

Constituent	Fe_2O_3	Al_2O_3	SiO_2	TiO_2	CaO	Na_2O
wt.%	42.45	10.35	6.89	-	0.72	1.36

The coal with the following characteristics was used as the reductant: fixed carbon—78.99%, volatile matter—7.4%, ash content—10.95%; sodium borate was used as an additive. Red mud, sodium borate (0–6 wt.%) and coal fines (7–12 wt.%) were blended using a small amount of water. Cylindrical briquettes were prepared in a mould by applying 8 MPa pressure for 1 min; these were then oven dried at 105 °C for 4 h. The reduction of briquettes was carried out in the temperature range 1200–1350 °C four times between 20 to 30 min in N_2 (1 L/min) atmosphere. Optimal roasting conditions were determined to be 1300 °C for 30 min. Reduced briquettes were ground finely, and the iron content was separated using magnetic separation (0.08 T). The addition of sodium borate was found to increase the iron grade of the recovered metallic powder to ~90%; which was attributed to the iron oxide reduction and the growth of metallic grains leading to an improved separation from gangue during subsequent magnetic processing.

4.2.3. Case Study 6

Zhang et al. [144] reported a semi-smelting reduction on an iron rich bauxite ore and magnetic separation process for the recovery of iron and alumina slag under a lower basicity condition. The composition of iron rich bauxite from western Guangxi, China is given in Table 6.

Table 6. Chemical composition of red mud [144].

Constituent	Fe_2O_3	Al_2O_3	SiO_2	TiO_2	CaO	Na_2O	LOI
wt.%	40.62	26.53	11.77	1.57	1.38	-	16.42%

Iron rich bauxite, $Ca(OH)_2$, anthracite coal, and CaF_2 were mixed thoroughly in a range of proportions and crushed using a ball mill. The anthracite coal with 78.73% fixed carbon was from Yangquan in Shanxi province in China. The average particle size and specific surface area of blends were determined to be 88.431 μm and 0.149 m^2/g. The mixtures were placed in a roller press and squeezed in the form of briquettes; these were then dried at 200 °C for 3 h. The composite briquettes were placed in a corundum crucible and reduced to a semi-smelting stage in a high temperature furnace in Ar (1.5 L/min) atmosphere. The reduction process was repeated three times. The reduced briquettes were crushed by the jaw crusher to 1–10 mm sizes and iron nugget and alumina slag were magnetically separated by a high strength magnetic field (0.4 T). Increasing the temperature can significantly increase the iron recovery and total iron content in the magnetic fraction; it also has a strong influence on the slag melting point and metallization rate of the briquettes. Reduction studies were carried out in the temperature range 1375–1450 °C for 1 to 15 min. Optimum conditions were determined to be: $w(CaO)/w(SiO_2)$ ratio of 1.25; 1425 °C, 15 min, anthracite proportion of ~12%. High quality iron nugget and high-grade alumina slag could be achieved with highest iron recovery rate (96.84 wt.%) and grade of alumina slag (43.98 wt.%), respectively.

4.2.4. Case Study 7

Guo et al. [145] used red mud from a Chinese aluminum plant and used magnetic separation to concentrate into iron rich fraction. The chemical composition of the iron rich RM is given in Table 7.

Table 7. Chemical composition of red mud [145].

Constituent	Fe$_2$O$_3$	Al$_2$O$_3$	SiO$_2$	TiO$_2$	CaO	Na$_2$O
wt.%	63.2	8.96	8.54	-	0.551	2.5

Red mud, anthracite coal, and lime-stone were used as raw materials; these were baked in a drying cabinet with forced convection at 200 °C for 2 h. These were mixed in a range of proportion to ensure sufficient carbon reductant and desired basicity. The mixture was homogenized with a binder and compacted into pellets using a roller press. Direct reduction of pellets was carried out in a muffle furnace using following operating conditions: 1350 °C/20 min; 1375 °C/25 min; and 1400 °C/30 min. Heat treated pellets were quenched in liquid N$_2$. The degree of metallization was determined using x-ray diffraction and chemical analysis. Temperature was found to be a key factor for reduction and the separation of metal and slag. Iron nuggets with an iron content of 96.52 wt.% were observed within the pellets after 1400 °C/30 min heat treatment. A chemical analysis of nuggets showed that the total iron was higher than in pig iron along with lower Si and Mn contents.

4.3. GREECE

4.3.1. Case Study 8

Samouhos et al. [146] carried out investigations on red mud supplied by the Greek aluminum producer "Aluminum of Greece S.A". The RM was relatively finely grained with 60 wt.% of particles with sizes below 100 µm and 97 wt.% with particles below 400 µm. The chemical composition of the RM is given in Table 8.

Table 8. Chemical composition of red mud [146].

Constituent	Fe$_2$O$_3$	Al$_2$O$_3$	SiO$_2$	TiO$_2$	CaO	Na$_2$O	LOI
wt.%	43.59	18.45	6.0	5.54	11.38	1.82	11.7%

This study investigated the separation of the iron oxide from RM using low temperature reduction by hydrogen under static conditions, followed by wet magnetic separation. 20 gm of dried red mud sample (105 °C overnight) was placed in an alumina crucible and positioned in the outer region of a horizontal furnace (room temperature). The furnace tube was continuously purged with N$_2$ gas (250 mL/min) to remove all oxygen present. The sample was then transferred to the central hot zone and the gas flow switched from N$_2$ to N$_2$/H$_2$ gas mixtures in a range of proportions. RM samples were reduced in the temperature range 300–450 °C for 30 min and were furnace cooled by withdrawing to the outer region. The conversion degree of hematite to magnetite was investigated as a function of reduction time, temperature, and H$_2$ supply. A maximum conversion of 87% was achieved at 480 °C. Reduced RM samples were subjected to magnetic separation yielding a magnetic fraction with over 54 wt.% magnetite content.

4.3.2. Case Study 9

Cardenia et al. [147] carried out investigations on the RM provided by Mytilineos, Metallurgy Business Unit (formerly known as AoG). The particle size distribution of the dried sample had a mean particle size (D$_{50}$) of 1.87 µm and D$_{90}$ of 90% of the particles below 43 µm. The composition of red mud is given in Table 9.

Table 9. Chemical composition of red mud [147].

Constituent	Fe$_2$O$_3$	Al$_2$O$_3$	SiO$_2$	TiO$_2$	CaO	Na$_2$O	LOI
wt.%	43.51	19.25	6.5	5.49	9.58	2.80	9.41%

Dried homogenized bauxite residue was mixed with Na$_2$CO$_3$ in the ratio 4:1 and sintered in a muffle furnace at 900 °C for 2 h and furnace cooled. The sinter was stirred in a

0.1 M NaOH solution at 80 °C for 4 h with a 1.5% w/v pulp density and 240 rpm speed. Sodium and aluminum were leached out and a solid residue was left behind as modified red mud. The dried modified red mud was mixed with metallurgical coke in the ratio 4:9 and formed into pellets. These were roasted in a microwave at 600 W power, 300 s, and a N_2 gas flow of 1 L/min for three times. During the 1st and 2nd MW reductive roasting process, the resulting cinders were found to be rich in spherical metallic Fe particles trapped within the matrix. These were separated using a manual sieve. These were then subjected to a wet high intensity magnetic separation. A high concentration of metallic iron was detected in the magnetic fraction (56 wt.%) along with calcium, silicon, and titanium also present in minor quantities. Up to 4% iron was detected in the non-magnetic fraction. With successive MW roastings, the recovery of iron was further enhanced up to 69%.

4.3.3. Case Study 10

Borra et al. [107] used the red mud provided by the Aluminum of Greece Company (Agios Nikolaos, Greece). The composition of RM is provided in Table 10.

Table 10. Chemical composition of red mud [107].

Constituent	Fe_2O_3	Al_2O_3	SiO_2	TiO_2	CaO	Na_2O
wt.%	44.6	23.6	10.2	5.7	11.2	2.5

The RM sample was mixed with graphite (5–15 wt.%) and flux using a pestle and mortar; wollastonite ($CaSiO_3$) was used as a flux and graphite as a reducing agent. Handmade pellets were dried at 105 °C for 12 h. Smelting reduction experiments were carried out in a high-temperature vertical alumina tube furnace in the temperature range 1500–1600 °C with a heating rate 5 °C/min and kept at the pre-set temperature for 1 h. High purity Ar gas was flushed through the furnace at a flow rate of 0.4 L/min. After the heat treatment, the furnace was cooled down to room temperature. Optimum conditions at 1500 °C were identified as 20 wt.% wollastonite and 5 wt.% of graphite. More than 85 wt.% iron could be separated in the form of a nugget. Additional 10% iron could be recovered through subsequent grinding of slag and magnetic separation.

4.4. ITALY

Case Study 11

Mombelli et al. [124] used red muds from EurAllumina S.p.A., Portovesme (Italy) as a raw material for the production of iron-based secondary raw material in the form of cast iron and direct reduced iron (DRI). The composition of fresh and calcined red mud is given in Table 11. Red muds were calcined in a muffle furnace at 1000 °C for 60 min to eliminate hydroxide and carbonate species. Graphite and blast furnace sludge were used as reducing agents; lime was added as a fluxing agent to aid slag formation.

Table 11. Chemical composition of red mud [124].

Constituent (wt.%)	Fe_2O_3	Al_2O_3	SiO_2	TiO_2	CaO	Na_2O	LOI
Fresh RM	20.89	16.3	9.8	5.2	5.54	10.39	29.78
Calcined RM	28.26	21.05	15.69	7.26	7.69	13.44	3.78

A muffle furnace was used to carry out reduction experiments at 1200 °C, 1300 °C, and 1500 °C. The furnace containing the samples was heated to these temperature, maintained for 15 min, and then cooled. The results showed that the blast furnace sludge was a suitable reductant to recover the iron fraction in the red mud. The metallization degree achieved was higher than 70%; the composition 1:1 red mud/blast furnace sludges were found to be equivalent to 0.85 C/Fe_2O_3. Mombelli et al. [148] mixed RM with 6 and 12 wt.% metallurgical coke and slag conditioners CaO and SiO_2 and reduced the blend in an arc transferred plasma (ATP) reactor at 1600–1700 °C for 30–35 min. The quality of cast iron quality produced was evaluated for sake of valorization and marketability.

4.5. FRANCE

Case Study 12

Maihatchi et al. [149] have used an alternative route to beneficiate RM by directly producing electrolytic iron from hematite present in red muds in a highly alkaline medium. Red mud specimens were obtained from Alteo, a European alumina manufacturer. The chemical composition of RM is provided in Table 12.

Table 12. Chemical composition of red mud [149].

Constituent	Fe_2O_3	Al_2O_3	SiO_2	TiO_2	CaO	Na_2O
wt.%	52.7	13.9	4.19	7.4	4.1	2.1

A double-walled Pyrex cell with a total volume of 600 mL and diameter 80 mm was used in the experiments. Approximately 450 mL of 12.5 mol/L NaOH solution and 150 g of red mud were introduced into the cell. A cylindrical graphite rod with a 19.4 cm^2 wetted area was used as the working electrode. A platinum-coated titanium grid was used as a counter electrode. A saturated Ag/AgCl electrode was used as the reference electrode. A SP-150 potentiostat coupled to a 10 A booster acted as the current source. The solid: liquid ratio and amounts of impurities present in red mud were varied to optimize the faradaic yield and the production rate of electrolytic iron. Hematite could be reduced to iron with an efficiency over 80% for current densities up to 1000 A/m^2. Highest current efficiency for red muds were achieved for current densities below 50 A/m^2; these efficiencies were seen to decrease to 20% at 1000 A/m^2. The produced electrodeposit contained more than 97% metal iron in all cases. For the economic and commercial viability of this technique, it is requisite to obtain larger faradaic yields for the beneficiation process.

4.6. RUSSIA

4.6.1. Case Study 13

Valeev et al. [119] carried out reductive smelting on neutralized RM from Ural Aluminium Plant (Kamensk-Uralsky, Russia) with an aim to obtain the maximum amount of pig iron and to achieve a complete separation of the metal and slag. The chemical composition of RM is given in Table 13.

Table 13. Chemical composition of red mud [119].

Constituent	Fe_2O_3	Al_2O_3	SiO_2	TiO_2	CaO	Na_2O	LOI
wt.%	36.9	11.8	8.71	3.54	23.8	0.27	12.46%

The mixture with 27.6 g RM and 2.4 g graphite was loaded in a carbon crucible and placed in a Tammann furnace for reductive smelting. The furnace was heated up to 1300 °C rapidly for 1 h, then a slow heating to the required temperature range 1650–1750 °C at 10 °C/min. The assembly was kept at these temperatures for 10 min. The furnace was then switched off and the crucibles were furnace cooled to room temperature. After 1650 °C smelting reduction, the slag phase containing up to 8% Fe was not separated from the metal. Increasing temperature to 1700 °C saw the iron content in the slag to reduce to ~3% and the formation of large metal ingots at the crucible bottom. Almost complete separation of metal and slag was observed at 1750 °C with the iron content in the slag dropping to 0.16%. Pig iron obtained at 1750 °C could find application for producing moulds for steel-casting.

4.6.2. Case Study 14

Grudinsky et al. [150] have reported on the solid-state carbothermic roasting of two RMs in the presence of special additives followed by magnetic separation. Red muds were obtained from Bogoslovsky Aluminum Plant (Russian Federation, labelled as 'B') and from the Ural Aluminum Plant (Russian Federation, labelled as 'U'). The composition of 'B' and 'U' RMs are provided in Tables 13 and 14 respectively.

Table 14. Chemical composition of red mud [150].

Constituent	Fe$_2$O$_3$	Al$_2$O$_3$	SiO$_2$	TiO$_2$	CaO	Na$_2$O
wt.%	49.81	12.77	8.71	4.67	9.26	33

Long-flaming coal with 15% ash content and 18% moisture content was used as a reductant; Na$_2$SO$_4$ was used as an additive. RM, coal, and the additive were finely ground and blended together. These blends were roasted in a muffle furnace in the temperature range 1000–1450 °C, for times between 20–180 min. Heat treated samples were removed from the furnace and quenched with liquid N$_2$. Roasted RM samples were ground finely, and the iron rich fraction was magnetically separated using a magnetic field of 0.35 T. Iron concentrates with more than 95% of iron recovery and 83% of the iron grade were obtained for 'U' and 'B' red muds respectively. Optimal conditions for the roasting of the samples were a duration of 180 min with the addition of 13.65% Na$_2$SO$_4$ at 1150 °C and 1350 °C for the 'B' and the 'U' RMs respectively.

5. Comparison with Low Grade Iron Ores

The overall quality of an iron ore is judged mainly by its Fe content in the elemental form. Iron ores with Fe contents above 65% are considered high-grade ores [35,151]. Medium grade ores contain ~62–64% iron and those below 58% iron are low grade ores. Other important considerations include the concentrations of SiO$_2$, Al$_2$O$_3$, and S and P. The alumina to silica ratio higher than one can cause serious operational problems during sintering and subsequent smelting in the blast furnace [152]. High alumina content in the iron ore/and sinter leads to a viscous slag during smelting in a blast furnace resulting in a high consumption of coke as well as other concerns during tapping. Generalized concentrations of SiO$_2$ in iron ore should be less than 6 wt.% [153] and Al$_2$O$_3$ should be between 3–4 wt.%. [154] for blast furnace ironmaking.

In Figure 1, the Fe$_2$O$_3$, Al$_2$O$_3$, and SiO$_2$ contents of RMs from the 14 case studies have been plotted. The Fe$_2$O$_3$ content in most cases was between 30–50 wt.%; the average value was determined to be ~44 wt.%. The Al$_2$O$_3$ content of various RMs was quite high ranging between 6.9 to 26.5 wt.%; the SiO$_2$ content ranged between 2.3 to 22 wt.%.

In Figure 2, Al$_2$O$_3$/SiO$_2$ ratio vs. Fe$_2$O$_3$ content has been plotted for various red muds. Except for one RM, this ratio was higher than 1 (range: 1.3 to 4.6) for most RMs under investigation. Low Al$_2$O$_3$ in the iron ore facilitates and helps in maintaining lower alumina in slag without increasing slag rate and keeping it fluid. However, in sponge iron making (DRI) the SiO$_2$/Al$_2$O$_3$ ratio should preferably be 1. Higher SiO$_2$ in ore causes accretion formation in the DRI kiln; a balanced Al$_2$O$_3$ content enables easy dislodging of formed accretions. Some operations in China currently run on very high alumina iron ore, but the silica content is usually 3–4 times that of alumina.

China is currently world's largest producer of iron and produced 1053 Mt out of total global production of 1864 Mt [33,155]. Facing the risks of raw material shortages, China is working towards the feasibility of using domestic low grade/refractory iron ore resources. There is a large deposit in the Guangxi Zhuang Autonomous Region with an average of 43 wt.% Fe$_2$O$_3$ and 25 wt.% Al$_2$O$_3$ [156]. Rath et al. [157] have reported on a low grade iron ore from India containing 51.6 wt.% Fe$_2$O$_3$, 17.6 wt.% SiO$_2$ and 4.3 wt.% Al$_2$O$_3$.

In this study, iron recovery from a wide variety of red muds across the globe was reviewed in the form of case studies. Alumina content was higher than 20 wt.% in four case studies. In the case study 2 (Fe$_2$O$_3$: 47.9 wt.%; Al$_2$O$_3$: 22.64 wt.%; SiO$_2$: 10.25 wt.%; Al$_2$O$_3$/SiO$_2$: 1.92), the carbothermal reduction was carried out in muffle as well as microwave furnaces. Optimal conditions for iron recovery were determined as: muffle furnace: (1000 °C, 16.5 wt.% C, 50 min; 850 °C, 11 wt.% C, 50 min) and microwave furnace: (1000 °C, 11 wt.% C, 10 min and 850 °C, 5.5 wt.% C, 30 min). In case study 6 (Fe$_2$O$_3$: 40.6 wt.%; Al$_2$O$_3$: 26.53 wt.%; SiO$_2$: 11.77 wt.%; Al$_2$O$_3$/SiO$_2$: 2.25), high quality iron nuggets could be recovered with high iron recovery rate (96.84 wt.%) using semi-smelting reduction and magnetic separation process. In case study 10 (Fe$_2$O$_3$: 44.6 wt.%; Al$_2$O$_3$: 23.6 wt.%; SiO$_2$:

10.2 wt.%; Al_2O_3/SiO_2: 2.31), the smelting reduction experiments were carried out in the temperature range 1500–1600 °C; more than 85 wt.% iron could be recovered in the form of nuggets. In case study 11 (Fe_2O_3: 28.3 wt.%; Al_2O_3: 21.1 wt.%; SiO_2: 15.7 wt.%; Al_2O_3/SiO_2: 1.34), RM was mixed with 6 and 12 wt.% metallurgical coke and reduced in an arc transferred plasma (ATP) reactor at 1600–1700 °C for 30–35 min to achieve a high degree of metallization.
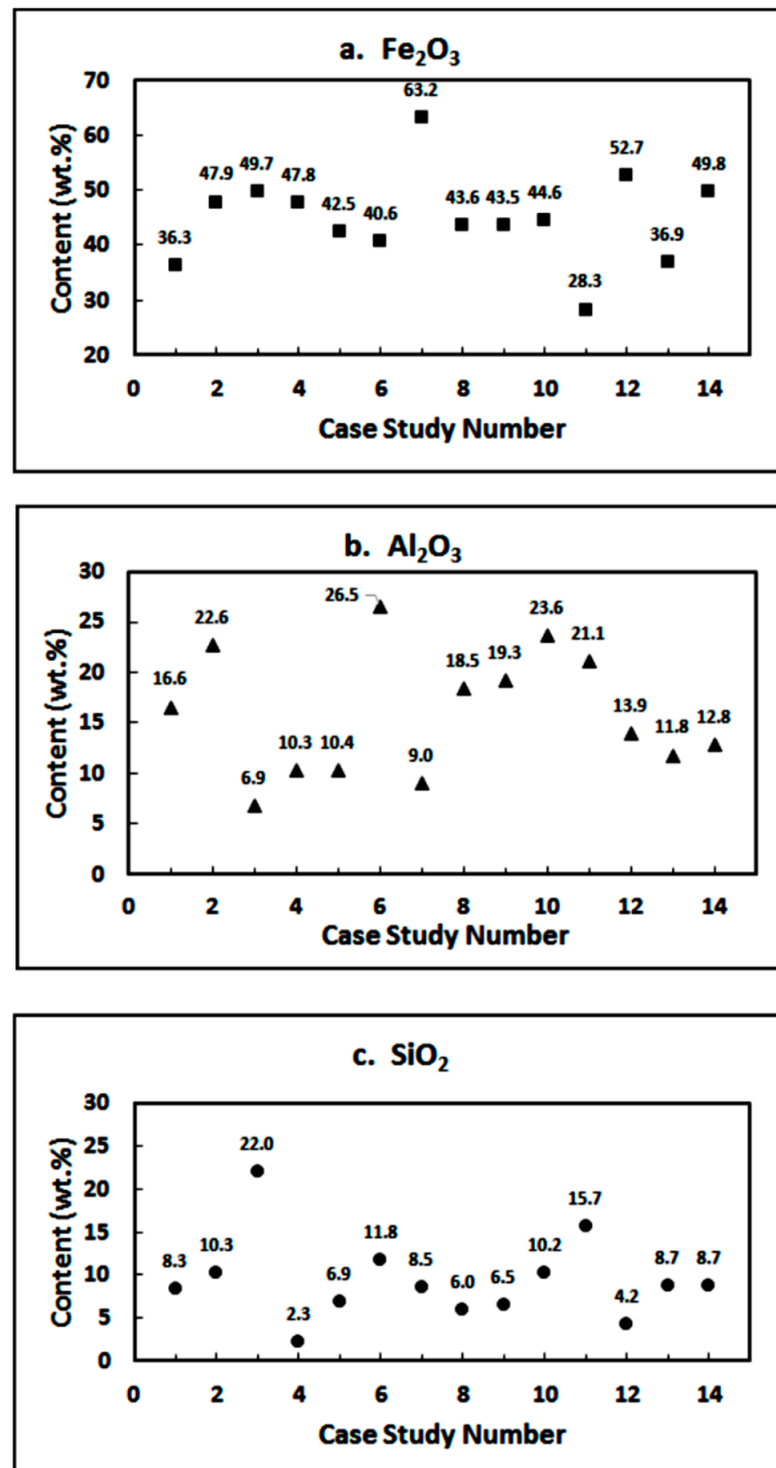

Figure 1. Concentrations of Fe_2O_3, Al_2O_3 and SiO_2 in red muds from case studies 1–14.
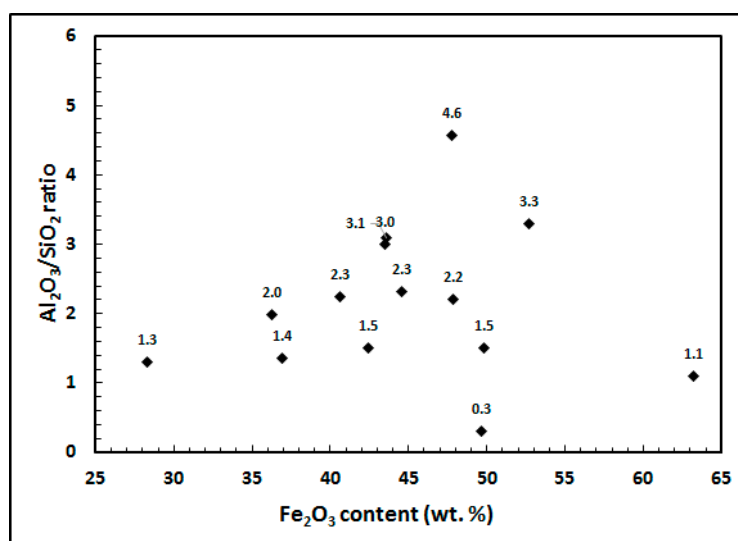
Figure 2. Al_2O_3/SiO_2 ratio vs. Fe_2O_3 concentration for red muds in case studies 1–14.

6. Concluding Remarks

In this article, we have focused our attention on evaluating the iron resource potential of RM. No attempt has been made towards establishing policies for managing RM waste or measures for a circular economy. Iron ore resources are getting consumed at a fast rate leading to a reduced availability of high-grade iron ores; the current scenario is steadily shifting towards the use of low-grade iron ores. Key findings from this study indicate that even with high levels of Al_2O_3 and SiO_2, red muds have a good potential to be used as a low-grade iron resource.

While RMs may not qualify as suitable blast furnace feed, these can find application as iron resource in DRIs, iron nuggets, sinters, etc. Alternatively, the blending of ores and waste products could play a significant role in the selection process. An economic and sustainable iron recovery operations may require more than a single feed source. Such an approach has been successfully used to partially replace coal/coke with waste carbonaceous products in iron and steelmaking [158,159]. Along with supplementing the natural resource sector, waste reutilization will enhance the environmental sustainability of materials sector, resource conservation, as well as reducing the carbon footprint of the industry.

Author Contributions: Conceptualization, original draft: R.K. and Y.K.; Supervision and resources: D.Z., K.J. and I.B. Formal analysis: M.K. and P.S.M. All authors have read and agreed to the published version of the manuscript.

Institutional Review Board Statement: Not applicable.

Informed Consent Statement: Not applicable.

Conflicts of Interest: The authors declare no conflict of interest.

References

1. Zhang, R.; Zheng, S.; Ma, S.; Zhang, Y. Recovery of alumina and alkali in Bayer red mud by the formation of andradite-grossular hydrogarnet in hydrothermal process. *J. Hazard. Mater.* **2011**, *189*, 827–835. [CrossRef]
2. Archambo, M.; Kawatra, S.K. Red mud: Fundamentals and new avenues for utilization. *Miner. Process. Extr. Metall. Rev.* **2020**, *42*, 427–450. [CrossRef]
3. Yu, H.; Pan, X.; Dong, K.; Zhang, W.; Bi, S. The Sintering and Leaching of Low-Grade Diasporic Bauxite by the Improved Lime-Sintering Process. *Adv. Mater. Res.* **2013**, *616–618*, 1051–1054. [CrossRef]
4. Wang, P.; Liu, D.Y. Physical and Chemical Properties of Sintering Red Mud and Bayer Red Mud and the Implications for Beneficial Utilization. *Materials* **2012**, *5*, 1800–1810. [CrossRef]

5.   Feng, Y.; Yang, C. Analysis on Physical and Mechanical Properties of Red Mud Materials and Stockpile Stability after Dilatation. *Adv. Mater. Sci. Eng.* **2018**, *2018*, 8784232. [CrossRef]

6.   Patel, S.; Pal, B.K. Current Status of an Industrial Waste: Red Mud an Overview. *IJLTEMAS* **2015**, *7*, 1–16.

7.   Wang, L.; Sun, N.; Tang, H.; Sun, W. A review on comprehensive utilization of red mud and prospect analysis. *Minerals* **2019**, *9*, 362. [CrossRef]

8.   Boudreault, R.; Fournier, J.; Primeau, D.; Labrecque-Gilbertm, M.M. Processes for Treating Red Mud. US20150275330A1, 31 January 2017.

9.   Xue, S.; Wu, Y.; Li, Y.; Kong, X.; Zhu, F.; William, H.; Li, X.; Ye, Y. Industrial wastes applications for alkalinity regulation in bauxite residue: A comprehensive review. *J. Cent. South Univ.* **2019**, *26*, 268–288. [CrossRef]

10. Arroyo, F.; Luna-Galiano, Y.; Leiva, C.; Vilches, L.F.; Fernandez-Pereira, C. Environmental risks and mechanical evaluation of recycling red mud in bricks. *Environ. Res.* **2020**, *186*, 109537. [CrossRef]

11. Khairul, M.A.; Zanganeh, J.; Moghtaderi, B. The composition, recycling and utilisation of Bayer red mud. *Resour. Conserv. Recyc.* **2019**, *141*, 483–498. [CrossRef]

12. Garg, A.; Yadav, H. Study of red mud as an alternative building material for interlocking block manufacturing in construction industry. *Int. J. Mater. Sci. Eng.* **2015**, *3*, 295–300.

13. Paramguru, R.K.; Rath, P.C.; Misra, V.N. Trends in red mud utilization: A review. *Miner. Process. Extr. Metall. Rev.* **2004**, *26*, 1–29. [CrossRef]

14. Wang, S.; Ang, H.M.; Tade, M.O. Novel applications of red mud as coagulant, adsorbent and catalyst for environmentally benign processes. *Chemosphere* **2008**, *72*, 1621–1635. [CrossRef]

15. Liu, X.; Han, Y.; He, F.; Gao, P.; Yuan, S. Characteristic, hazard and iron recovery technology of red mud—A critical review. *J. Hazard. Mater.* **2021**, *420*, 126542. [CrossRef]

16. Snars, K.; Gilkes, R.J. Evaluation of bauxite residues (red muds) of different origins for environmental applications. *Appl. Clay Sci.* **2009**, *46*, 13–20. [CrossRef]

17. Klauber, C.; Grafe, M.; Power, G. Bauxite residue issues: II. options for residue utilization. *Hydrometallurgy* **2011**, *108*, 11–32. [CrossRef]

18. Piga, L.; Pochetti, F.; Stoppa, L. Recovering metals from red mud generated during alumina production. *JOM* **1993**, *45*, 54–59. [CrossRef]

19. Rai, S.; Bahadure, S.; Chaddha, M.J.; Agnihotri, A. Disposal practices and utilization of red mud (Bauxite Residue): A review in Indian context and abroad. *J. Sustain. Metall.* **2020**, *6*, 1–8. [CrossRef]

20. Das, B.; Mohanty, K. A review on advances in sustainable energy production through various catalytic processes by using catalysts derived from waste red mud. *Renew. Energy* **2019**, *143*, 1791–1811. [CrossRef]

21. Liu, Y.; Lin, C.; Wu, Y. Characterization of red mud derived from a combined Bayer process and bauxite calcination method. *J. Hazard. Mater.* **2007**, *146*, 255–261. [CrossRef]

22. Mayes, W.M.; Jarvis, A.P.; Burke, I.T.; Walton, M.; Feigl, V.R.; Klebercz, O.; Gruiz, K. Dispersal and attenuation of trace contaminants downstream of the Ajka bauxite residue (red mud) depository failure. *Hung. Environ. Sci. Technol.* **2011**, *45*, 5147–5155. [CrossRef] [PubMed]

23. Wang, W.; Pranolo, Y.; Cheng, C.Y. Recovery of scandium from synthetic red mud leach solutions by solvent extraction with D2EHPA. *Sep. Purif. Technol.* **2013**, *108*, 96–102. [CrossRef]

24. Ruyters, S.; Mertens, J.; Vassilieva, E.; Dehandschutter, B.; Poffijn, A.; Smolders, E. The Red Mud Accident in Ajka (Hungary): Plant Toxicity and Trace Metal Bioavailability in Red Mud Contaminated Soil. *Environ. Sci. Technol.* **2011**, *45*, 1616–1622. [CrossRef]

25. Kumar, S.; Kumar, R.; Bandopadhyay, A. Innovative methodologies for the utilisation of wastes from metallurgical and allied industries. *Resour. Conserv. Recycl.* **2006**, *48*, 301–314. [CrossRef]

26. Liu, Z.; Li, H. Metallurgical process for valuable elements recovery from red mud—A review. *Hydrometallurgy* **2015**, *155*, 29–43. [CrossRef]

27. Pascual, J.; Corpas, F.; López-Beceiro, J.; Benítez-Guerrero, M.; Artiaga, R. Thermal characterization of a Spanish red mud. *J. Therm. Anal. Calorim.* **2009**, *96*, 407–412. [CrossRef]

28. Samal, S.; Ray, A.K.; Bandopadhyay, S.A. Proposal for resources, utilization and processes of red mud in India—A review. *Int. J. Miner. Process.* **2013**, *118*, 43–55. [CrossRef]

29. Evans, K. The History, Challenges, and New Developments in the Management and Use of Bauxite Residue. *J. Sustain. Met.* **2016**, *2*, 316–331. [CrossRef]

30. Bonomi, C.; Giannopoulou, I.; Panias, D. Correlation of Scandium and Titanium during Leaching of Bauxite Residue (Red Mud) by an Imidazolium Ionic Liquid. In *Proceedings of the 2nd Conference on European Rare Earth Resources*; Balomenos, E., Marinos, D., Eds.; Heliotopos Conferences Ltd.: Santorini, Greece, 2017; pp. 182–184.

31. Sutar, H.; Mishra, S.C.; Sahoo, S.K.; Maharana, H. Progress of red mud utilization: An overview. *Am. Chem. Sci. J.* **2014**, *4*, 255–279. [CrossRef]

32. Liu, Y.; Naidu, R. Hidden values in bauxite residue (red mud): Recovery of metals. *Waste Manag.* **2014**, *34*, 2662–2673. [CrossRef] [PubMed]

33. Steel industry—Statistics & Facts. Available online: https://www.statista.com/topics/1149/steel-industry/ (accessed on 30 November 2021).

34. Kumar, R.; Srivastava, J.P.; Premchand. Utilization of iron values of red mud for metallurgical applications. In *Environmental and Waste Management*; Bandopadhyay, A., Goswami, N.G., Jamshedpur, P.R.R., Eds.; National Metallurgical laboratories: Jamshedpur, India, 1998; pp. 108–119.

35. Sparks, B.D.; Sirianni, A.F. Beneficiation of a phosphoriferous iron ore by agglomeration methods. *Int. J. Miner. Process.* **1974**, *1*, 231–241. [CrossRef]

36. Bao, Q.; Guo, L.; Guo, Z. A novel direct reduction-flash smelting separation process of treating high phosphorous iron ore fines. *Powder Metall.* **2021**, *377*, 149–162. [CrossRef]

37. Jorgen, D.J. U.S. Geological Survey, Mineral Commodities Summary. Available online: https://minerals.usgs.gov/minerals/pubs/commodity/ironore/mcs-2010-feore.pdf (accessed on 28 November 2020).

38. Muwanguzi, A.J.B.; Karasev, A.V.; Byaruhanga, J.K.; Jönsson, P.G. Characterization of Chemical Composition and Microstructure of Natural Iron Ore from Muko Deposits. *Int. Sch. Res. Notices* **2012**, *2012*, 174803. [CrossRef]

39. Agrawal, A.; Sahu, K.K.; Pandey, B.D. Solid waste management in non-ferrous industries in India. *Resour. Conserv. Recycl.* **2004**, *42*, 99–102. [CrossRef]

40. Abhilash; Sinha, S.; Sinha, M.K.; Pandey, B.D. Extraction of lanthanum and cerium from Indian red mud. *Int. J. Miner. Process.* **2014**, *127*, 70–73. [CrossRef]

41. Mukiza, E.; Zhang, L.; Liu, X.; Zhang, N. Utilization of red mud in road base and subgrade materials: A review. *Resour. Conserv. Recycl.* **2019**, *141*, 187–199. [CrossRef]

42. Pontikes, Y.; Angelopoulos, G.N. Bauxite residue in cement and cementitious applications: Current status and a possible way forward. *Resour. Conserv. Recycl.* **2013**, *73*, 53–63. [CrossRef]

43. Feng, X.-p.; Liu, X.-m.; Sun, H.-h.; Bai, X.; Niu, X.-l. Study on the High Use Ratio of Red Mud in Cementitious Material. *Multipurpose Util. Miner. Resour.* **2007**, *4*, 35–37.

44. Liu, R.-X.; Poon, C.-S. Utilization of red mud derived from bauxite in self-compacting concrete. *J. Clean. Prod.* **2016**, *112*, 384–391. [CrossRef]

45. Nikbin, I.M.; Aliaghazadeh, M.; Sh, C.; Fathollahpour, A. Environmental impacts and mechanical properties of lightweight concrete containing bauxite residue (red mud). *J. Clean. Prod.* **2018**, *172*, 2683–2694. [CrossRef]

46. Kacker, K.P.; Chandra, D. Production of building bricks from red mud rejects of aluminium plants. *Ind. Ceram.* **1977**, *19*, 712–723.

47. Prasad, P.M.; Kachhawha, J.S.; Gupta, R.C.; Mankhand, T.R.; Sharma, J.M. Processing and Applications of Red Muds. In *Key Engineering Materials*; Trans Tech Publications Ltd.: Bäch, Switzerland, 1985; Volume 8, pp. 31–52.

48. Dodoo-Arhin, D.; Konadu, D.S.; Annan, E.; Buabeng, F.P.; Yaya, A.; Agyei-Tuffour, B. Fabrication and Characterisation of Ghanaian Bauxite Red Mud-Clay Composite Bricks for Construction Applications. *Am. J. Mater. Sci.* **2013**, *3*, 110–119.

49. Alam, S.; Das, S.K.; Rao, B.H. Characterization of coarse fraction of red mud as a civil engineering construction material. *J. Clean. Prod.* **2017**, *168*, 679–691. [CrossRef]

50. Wang, L.; Iris, K.M.; Tsang, D.C.W.; Li, S.; Li, J.; Poon, C.S.; Wang, Y.S.; Dai, J.G. Transforming wood waste into water-resistant magnesia-phosphate cement particleboard modified by alumina and red mud. *J. Clean. Prod.* **2017**, *168*, 452–462. [CrossRef]

51. Tang, W.C.; Wang, Z.; Donne, S.W.; Forghani, M.; Liu, Y. Influence of red mud on mechanical and durability performance of self-compacting concrete. *J. Hazard Mater.* **2019**, *379*, 120802. [CrossRef] [PubMed]

52. Kim, Y.; Kim, M.; Sohn, J.; Park, H. Applicability of gold tailings, waste lime stone, red mud, and ferronickel slag for producing glass fibers. *J. Clean. Prod.* **2018**, *203*, 957–965. [CrossRef]

53. Krivenko, P.; Kovalchuk, O.; Pasko, A.; Croymans, T.; Hult, M.; Lutter, G.; Vandevenne, N.; Schreurs, S.; Schroeyers, W. Development of alkali activated cements and concrete mixture design with high volumes of red mud. *Construct. Build. Mater.* **2017**, *151*, 819–826. [CrossRef]

54. Lemougna, P.N.; Wang, K.T.; Tang, Q.; Cui, X.M. Synthesis and characterization of low temperature (<800 °C) ceramics from red mud geopolymer precursor. *Construct. Build. Mater.* **2017**, *131*, 564–573. [CrossRef]

55. Yang, Z.; Mocadlo, R.; Zhao, M.; Sisson, R.D., Jr.; Tao, M.; Liang, J. Preparation of a geopolymer from red mud slurry and class F fly ash and its behavior at elevated temperatures. *Constr. Build. Mat.* **2019**, *221*, 308. [CrossRef]

56. Vigneshwaran, S.; Uthayakumar, M.; Arumugaprabu, V. Potential use of industrial waste-red mud in developing hybrid composites: A waste management approach. *J. Clean. Prod.* **2020**, *276*, 124278. [CrossRef]

57. Amritphale, S.S.; Anshul, A.; Chandra, N.; Ramakrishnan, N. A novel process for making radiopaque materials using bauxite-red mud. *J. Eur. Ceram. Soc.* **2007**, *27*, 1945–1951. [CrossRef]

58. Singh, B.; Gupta, M. Surface treatment of red mud and its influence on the properties of particulate-filled polyester composite. *Bull. Mater. Sci.* **1995**, *18*, 603–621. [CrossRef]

59. Hertel, T.; Cardenia, C.; Balomenos, E.; Panias, D.; Pontikes, Y. Microwave Treatment of Bauxite Residue for the Production of Inorganic Polymers. In Proceedings of the 2nd International Bauxite Residue Valorisation and Best Practices Conference, Athens, Greece, 7–10 May 2018.

60. Qin, S.; Wu, B. Effect of self-glazing on reducing the radioactivity levels of red mud based ceramic materials. *J. Hazard. Mater.* **2011**, *198*, 269–274. [CrossRef] [PubMed]

61. Yang, J.; Zhang, D.; Hou, J.; He, B.; Xiao, B. Preparation of glass-ceramics from red mud in the aluminium industries. *Ceram. Int.* **2008**, *34*, 125–130. [CrossRef]

62. Dry, C.; Meier, J.; Bukowski, J. Sintered coal ash/flux materials for building materials. *Mater. Struct.* **2004**, *37*, 114–121. [CrossRef]

63. Promentilla, M.A.B.; Thang, N.H.; Kien, P.T.; Hinode, H.; Bacani, F.T.; Gallardo, S.M. Optimizing Ternary-blended Geopolymers with Multi-response Surface Analysis. *Waste Biomass Valor.* **2016**, *7*, 929–939. [CrossRef]

64. Hertel, T.; Pontikes, Y. Geopolymers, inorganic polymers, alkali-activated materials and hybrid binders from bauxite residue (red mud)—Putting things in perspective. *J. Clean. Prod.* **2020**, *258*, 120610. [CrossRef]

65. Li, G.H.; Liu, M.X.; Rao, M.J.; Jiang, T.; Zhuang, J.Q.; Zhang, Y.B. Stepwise extraction of valuable components from red mud based on reductive roasting with sodium salts. *J. Hazard. Mater.* **2014**, *280*, 774–780. [CrossRef]

66. Yang, J.K.; Chen, F.; Xiao, B. Engineering application of basic level materials of red mud high level pavement. *China Munic. Eng.* **2006**, *5*, 7–9. [CrossRef]

67. Sushil, S.; Batra, V.S. Catalytic applications of red mud, an aluminium industry waste: A review. *Appl. Catal. B Environ.* **2008**, *81*, 64–77. [CrossRef]

68. Ordonez, S. Comments on catalytic applications of red mud, an aluminium industry waste: A review. *Appl. Catal. B Environ.* **2008**, *84*, 732–733. [CrossRef]

69. Bhatnagar, A.; Vilar, V.J.P.; Botelho, C.M.S.; Boaventura, R.A.R. A review of the use of red mud as adsorbent for the removal of toxic pollutants from water and wastewater. *Environ. Technol.* **2011**, *32*, 231–249. [CrossRef] [PubMed]

70. Ciccu, R.; Ghiani, M.; Serci, A.; Fadda, S.; Peretti, R.; Zucca, A. Heavy metal immobilization in the mining-contaminated soils using various industrial wastes. *Miner. Eng.* **2003**, *16*, 187–192. [CrossRef]

71. Chen, Y.; Li, J.-Q.; Huang, F.; Zhou, J.; Zhou, D.-F.; Liu, W. The performance research on absorbing SO_2 waste gas with Bayer red mud. *J. Guizhou Teachers Univ. Nat. Sci.* **2007**, *36*, 30–32.

72. Brunori, C.; Cremisini, C.; Massanisso, P.; Pinto, V.; Torricelli, L. Reuse of a treated red mud bauxite waste: Studies on environmental compatibility. *J. Hazard. Mater.* **2005**, *117*, 55–63. [CrossRef] [PubMed]

73. Zhang, J.Z.; Yao, Z.Y.; Wang, K.; Wang, F.; Jiang, H.G.; Liang, M.; Wei, J.C.; Airey, G. Sustainable utilization of bauxite residue (Red Mud) as a road material in pavements: A critical review. *Constr. Build Mater.* **2021**, *270*, 121419. [CrossRef]

74. Novais, R.M.; Carvalheiras, J.; Seabra, M.P.; Pullar, R.C.; Labrincha, J.A. Innovative application for bauxite residue: Red mud-based inorganic polymer spheres as pH regulators. *J. Hazard. Mater.* **2018**, *358*, 69–81. [CrossRef] [PubMed]

75. Ujaczki, E.; Feigl, V.; Molnár, M.; Cusack, P.; Curtin, T.; Courtney, R.; O'Donoghue, L.; Davris, P.; Hugi, C.; Evangelou, M.; et al. Re-using bauxite residues: Benefits beyond (critical raw) material recovery. *J. Chem. Technol. Biotechnol.* **2018**, *93*, 2498–2510. [CrossRef]

76. Grafe, M.; Power, G.; Klauber, C. Bauxite residue issues: III. Alkalinity and associated chemistry. *Hydrometallurgy* **2011**, *108*, 60–79. [CrossRef]

77. Narayanan, R.; Kazantzis, P.; Nikolaos, K.; Emmert, M.H. Selective process steps for the recovery of scandium from Jamaican bauxite residue (red mud). *ACS Sustain. Chem. Eng.* **2018**, *6*, 1478–1488. [CrossRef]

78. Guo, D.; Yang, G.; Chen, J.; Fan, Y.; Zhan, H.; Liang, H.; Li, B.; Man, L.; Zhang, J.; Rong, J.; et al. Method for Comprehensively Recovering Scandium and Titanium by Leaching Red Mud with Titanium White Waste Acid. CN103131854B, 28 August 2014.

79. Ochsenkühn-Petropulu, M.; Lyberopulu, T.; Parissakis, G. Direct determination of landthanides, yttrium and scandium in bauxites and red mud from alumina production. *Anal. Chim. Acta* **1994**, *296*, 305–313. [CrossRef]

80. Agrawal, S.; Dhawan, N. Evaluation of red mud as a polymetallic source—A review. *Miner. Eng.* **2021**, *171*, 107084.

81. Vachon, P.; Tyagi, R.D.; Auclair, J.C.; Wilkinson, K.J. Chemical and biological leaching of aluminium from red mud. *Environ. Sci. Technol.* **1994**, *28*, 26–30. [CrossRef]

82. Bruckard, W.J.; Calle, C.M.; Davidson, R.H.; Glenn, A.M.; Jahanshahi, S.; Somerville, M.A.; Sparrow, G.J.; Zhang, L. Smelting of bauxite residue to form a soluble sodium aluminium silicate phase to recover alumina and soda. Miner. Process. *Extract. Metall.* **2010**, *119*, 18–26.

83. Ablamoff, B.; Qian-de, C. *Physical and Chemical Principles of Comprehensive Treatment of Aluminium-containing Raw Materials by Basic Process*; Central South University of Technology Press: Changsha, China, 1988; pp. 178–182.

84. Kannan, P.; Banat, F.; Hasan, S.W.; Haija, M.A. Neutralization of Bayer bauxite residue (red mud) by various brines: A review of chemistry and engineering processes. *Hydrometallurgy* **2021**, *206*, 105758. [CrossRef]

85. Alp, A.; Selim Goral, M. The effects of the additives, calcination and leach conditions for alumina production from red mud. *Scand. J. Metall.* **2003**, *32*, 301–305. [CrossRef]

86. Meher, S.N.; Rout, A.K.; Padhi, B.K. Recovery of Al and Na values from red mud by $BaO-Na_2CO_3$ sinter process. *Eur. J. Chem.* **2011**, *8*, 1387–1393.

87. Agatzini-Leonardou, S.; Oustadakis, P.; Tsakiridis, P.E.; Markopoulos, C. Titanium leaching from red mud by diluted sulfuric acid at atmospheric pressure. *J. Hazard. Mater.* **2008**, *157*, 579–586. [CrossRef]

88. Erçag, E.; Apak, R. Furnace smelting and extractive metallurgy of red mud: Recovery of TiO2, Al2O3 and pig iron. *J. Chem. Technol. Biotechnol.* **1997**, *70*, 241–246. [CrossRef]

89. Huang, Y.; Chai, W.; Han, G.; Wang, W.; Yang, S.; Liu, J. A perspective of stepwise utilisation of Bayer red mud: Step two—extracting and recovering Ti from Ti enriched tailing with acid leaching and precipitate flotation. *J. Hazard. Mater.* **2016**, *307*, 318–327. [CrossRef]

90. Kasliwal, P.; Sai, P.S.T. Enrichment of titanium dioxide in red mud: A kinetic study. *Hydrometallurgy* **1999**, *53*, 73–87. [CrossRef]

91. Deep, A.; Malik, P.; Gupta, B. Extraction and separation of Ti(IV) using thiophosphinic acids and its recovery from ilmenite and red mud. *Sep. Sci. Technol.* **2001**, *36*, 671–685. [CrossRef]

92. Smirnov, D.I.; Molchanova, T.V. The investigation of sulphuric acid sorption recovery of scandium and uranium from the red mud of alumina production. *Hydrometallurgy* **1997**, *45*, 249–259. [CrossRef]

93. Davris, P.; Balomenos, E.; Panias, D.; Paspaliaris, I. Selective leaching of rare earth elements from bauxite residue (red mud), using a functionalized hydrophobic ionic liquid. *Hydrometallurgy* **2016**, *164*, 125–135. [CrossRef]

94. Lymperopoulou, T.; Georgiou, P.; Tsakanika, L.A.; Hatzilyberis, K.; Ochsenkuehn- Petropoulou, M. Optimizing conditions for scandium extraction from bauxite residue using taguchi methodology. *Minerals* **2019**, *9*, 236. [CrossRef]

95. Zhu, X.; Li, W.; Xing, B.; Zhang, Y. Extraction of scandium from red mud by acid leaching with CaF2 and solvent extraction with P507. *J. Rare Earths.* **2019**, *38*, 1003–1008. [CrossRef]

96. Alkan, G.; Yagmurlu, B.; Cakmakoglu, S.; Hertel, T.; Kaya, S.; Gronen, L.; Stopic, S.; Friedrich, B. Novel Approach for Enhanced Scandium and Titanium Leaching Efficiency from Bauxite Residue with Suppressed Silica Gel Formation. *Sci. Rep.* **2018**, *8*, 5676. [CrossRef] [PubMed]

97. Gu, H.; Li, W.; Li, Z.; Guo, T.; Wen, H.; Wang, N. Leaching Behaviour of Lithium from Bauxite Residue Using Acetic Acid. *Min. Metall. Explor.* **2020**, *37*, 443–451.

98. Panda, S.; Costa, R.B.; Shah, S.S.; Mishra, S.; Bevilaqua, D.; Ata Akcil, A. Biotechnological trends and market impact on the recovery of rare earth elements from bauxite residue (red mud)—A review. *Resour. Conserv. Recycl.* **2021**, *171*, 105645. [CrossRef]

99. Ochsenkuhn-Petropulu, M.; Lyberopulu, T.; Ochsenkuhn, K.M.; Parissakis, G. Recovery of lanthanides and yttrium from red mud by selective leaching. *Anal. Chim. Acta* **1996**, *319*, 249–254. [CrossRef]

100. Ujaczki, É.; Zimmermann, Y.S.; Gasser, C.A.; Molnár, M.; Feigl, V.; Lenz, M. Red mud as secondary source for critical raw materials–extraction study. *J. Chem. Technol. Biotechnol.* **2017**, *92*, 2835–2844. [CrossRef]

101. Shoppert, A.; Loginova, I.; Napol'skikh, J.; Kyrchikov, A.; Chaikin, L.; Rogozhnikov, D.; Valeev, D. Selective Scandium (Sc) Extraction from Bauxite Residue (RedMud Obtained by Alkali Fusion-Leaching Method. *Materials* **2022**, *15*, 433. [CrossRef]

102. Agrawal, S.; Dhawan, N. Investigation of carbothermic microwave reduction followed by acid leaching for recovery of iron and aluminium values from Indian red mud. *Miner. Eng.* **2020**, *159*, 106653. [CrossRef]

103. Chiara, B.; Chiara, C.; Tam, P.; WAI, T.; Dimitrios, P. Review of Technologies in the Recovery of Iron, Aluminium, Titanium and Rare Earth Elements from Bauxite Residue (Red Mud). In Proceedings of the 3rd International Symposium on Enhanced Landfill Mining, Lisbon, Portugal, 8–10 February 2016; pp. 259–276.

104. Stickney, W.A.; Butler, M.O.; Mauser, J.E.; Fursman, O.C. *Utilization of Red Mud Residues from Alumina Production*; US Department of Interior, Bureau of Mines: Washington, DC, USA, 1970.

105. Li, Y.; Wang, J.; Wang, X.; Wang, B.; Luan, Z. Feasibility study of iron mineral separation from red mud by high gradient superconducting magnetic separation. *Phys. C Supercond.* **2011**, *471*, 91–96. [CrossRef]

106. Rai, S.; Nimje, M.T.; Chaddha, M.J.; Modak, S.; Rao, K.R.; Agnihotri, A. Recovery of iron from bauxite residue using advanced separation techniques. *Miner. Eng.* **2019**, *2134*, 222–231. [CrossRef]

107. Borra, C.R.; Blanpain, B.; Pontikes, Y.; Binnemans, K.; Van Gerven, T. Smelting of bauxite residue (red mud) in view of iron and selective rare earths recovery. *J. Sustain. Metall.* **2016**, *22*, 28–37. [CrossRef]

108. Agrawal, S.; Dhawan, N. Microwave carbothermic reduction of low-grade iron ore. Metall. *Mater. Trans. B* **2020**, *51*, 1576–1586. [CrossRef]

109. Shuai, Y.; Xiao, L.; Peng, G.; Yuexin, H. A semi-industrial experiment of suspension magnetization roasting technology for separation of iron minerals from red mud. *J. Hazard. Mater.* **2020**, *394*, 122579.

110. Cardenia, C.; Balomenos, E.; Panias, D. Iron Recovery from Bauxite Residue through Reductive Roastingand Wet Magnetic Separation. *J. Sustain. Metall.* **2019**, *5*, 9–19. [CrossRef]

111. Wanchao, L.; Jiakuan, Y.; Xiao, B. Application of Bayer red mud for iron recovery and building material production from alumosilicate residues. *J. Hazard. Mater.* **2009**, *161*, 474–478.

112. Fanghai, L.; Xiangdong, S.; Fang, H.; Jiawei, W.; Haifeng, W. Co-Treatment of spent pot-lining and red mud for carbon reutilization and recovery of iron, aluminium and sodium by reductive roasting process. *Metall. Mater. Trans. B* **2020**, *51*, 1564–1575.

113. Agrawal, S.; Rayapudi, V.; Dhawan, N. Microwave reduction of red mud for recovery of iron values. *J. Sustain. Metall.* **2018**, *4*, 427–436. [CrossRef]

114. Agrawal, S.; Rayapudi, V.; Dhawan, N. Comparison of microwave and conventional carbothermal reduction of red mud for recovery of iron values. *Miner. Eng.* **2019**, *132*, 202–210. [CrossRef]

115. Javad, S.; Barani, K. Microwave Heating Applications in Mineral Processing. In *The Development and Application of Microwave Heating*; IntechOpen: Rijeka, Croatia, 2012; pp. 79–104.

116. Raspopov, N.A.; Korneev, V.P.; Averin, V.V.; Lainer, Y.A.; Zinoveev, D.V.; Dyubanov, V.G. Reduction of iron oxides during the pyrometallurgical processing of red mud. *Russ. Metall. Met.* **2013**, *1*, 33–37. [CrossRef]

117. Jayasankar, K.; Ray, P.K.; Chaubey, A.K.; Padhi, A.; Satapathy, B.K.; Mukherjee, P.S. Production of pig iron from red mud waste fines using thermal plasma technology. *Int. J. Miner. Metall. Mater.* **2012**, *19*, 679–684. [CrossRef]

118. Zhu, D.Q.; Chun, T.J.; Pan, J.; He, Z. Recovery of iron from high-iron red mud by reduction roasting with adding sodium salt. *Iron Steel Res. Int.* **2012**, *19*, 1–5. [CrossRef]

119. Valeev, D.; Zinoveev, D.; Kondratiev, A.; Lubyanoi, D.; Pankratov, D. Reductive smelting of neutralized red mud for iron recovery and produced pig iron for heat resistant castings. *Metals* **2020**, *10*, 32. [CrossRef]
120. Kaußen, F.; Friedrich, B. Reductive smelting of red mud for iron recovery. *Chem. Ing. Tech.* **2015**, *87*, 1535–1542. [CrossRef]
121. Kongkarat, S.; Khanna, R.; Koshy, O.; O'Kane, P.; Sahajwalla, V. Use of waste Bakelite as a raw material resource for re-carburization in steelmaking processes. *Steel Res. Int.* **2011**, *82*, 1228–1239. [CrossRef]
122. Shuai, L.; Zeshuang, K.; Wanchao, L.; Yicheng, L.; Hongshan, Y. Reduction behaviour and direct reduction kinetics of red mud-biomass composite pellets. *J. Sustain. Metall.* **2021**, *7*, 126–135.
123. Rahman, M.; Khanna, R.; Sahajwalla, V.; O'Kane, P. The influence of ash impurities on interfacial reactions between carbonaceous materials and EAF slag at 1550 °C. *ISIJ* **2009**, *49*, 329–336. [CrossRef]
124. Mombelli, D.; Barella, S.; Gruttadauria, A.; Mapelli, C. Iron Recovery from Bauxite Tailings Red Mud by Thermal Reduction with Blast Furnace Sludge. *Appl. Sci.* **2019**, *9*, 4902. [CrossRef]
125. Balomnenos, E.; Kastritis, D.; Panias, D.; Paspaliaris, I.; Boufounos, D. The Enexal Bauxite Residue Treatment Process: Industrial Scale Pilot Plant Results. In *Light Met*; Springer: Cham, Switzerland, 2014; pp. 141–147.
126. Jin, J.; Liu, X.; Yuan, S.; Gao, P.; Li, Y.; Zhang, H.; Meng, X. Innovative utilization of red mud through co-roasting with coal gangue for separation of iron and aluminium minerals. *J. Ind. Eng. Chem.* **2021**, *98*, 298–307. [CrossRef]
127. Cao, Y.; Sun, Y.; Gao, P.; Han, Y.; Li, Y. Mechanism for suspension magnetization roasting of iron ore using straw-type biomass reductant. *Int. J. Min. Sci. Technol.* **2021**, *31*, 1075–1081. [CrossRef]
128. Gostu, S.; Mishra, B.; Martins, G.P. Low Temperature Reduction of Hematite in Red Mud to Magnetite. In *Light Met*; Springer: Cham, Switzerland, 2017; pp. 67–73.
129. Liu, X.; Gao, P.; Yuan, S.; Yang, L.; Han, Y. Clean utilization of high-iron red mud by suspension magnetization roasting. *Miner. Eng.* **2020**, *157*, 106553. [CrossRef]
130. Yu, Z.; Shi, Z.; Chen, Y.; Niu, Y.; Wang, Y.; Wan, P. Red-mud treatment using oxalic acid by UV irradiation assistance. *Trans. Nonferrous Metal. Soc.* **2012**, *222*, 456–460. [CrossRef]
131. Debadatta, D.; Pramanik, K. A study on chemical leaching of iron from red mud using sulphuric acid. *Res. J. Chem. Environ.* **2013**, *17*, 50–56.
132. Pepper, R.A.; Couperthwaite, S.J.; Millar, G.J. Comprehensive examination of acid leaching behaviour of mineral phases from red mud: Recovery of Fe, Al, Ti, and Si. *Miner. Eng.* **2016**, *99*, 8–18. [CrossRef]
133. Yang, Y.; Xuewen, W.; Mingyu, W.; Huaguang, W.; Pengfei, X. Iron recovery from the leached solution of red mud through the application of oxalic acid. *Int. J. Miner. Process.* **2016**, *157*, 145–151. [CrossRef]
134. Eisele, T.C.; Gabby, K.L. Review of reductive leaching of iron by anaerobic bacteria. *Miner. Process. Extractive Metall. Rev.* **2014**, *35*, 75–105. [CrossRef]
135. Laguna, C.; Gonzalez, F.; Garcia-Balboa, C.; Ballester, A.; Blazquez, M.L.; Munoz, J.A. Bio-reduction of iron compounds as a possible clean environmental alternative for metal recovery. *Miner. Eng.* **2011**, *24*, 10–18. [CrossRef]
136. Papassiopi, N.; Vaxevanidou, K.; Paspaliaris, I. Effectiveness of iron reducing bacteria for the removal of iron from bauxite ores. *Miner. Eng.* **2010**, *23*, 25–31. [CrossRef]
137. Vakilchap, F.; Mousavi, S.M.; Shojaosadati, S.A. Role of Aspergillus niger in recovery enhancement of valuable metals from produced red mud in Bayer process. *Bioresour. Technol.* **2016**, *218*, 991–998. [CrossRef]
138. Qu, Y.; Lian, B. Bioleaching of rare earth and radioactive elements from red mud using Penicillium tricolor RM-10. *Bioresour. Technol.* **2013**, *136*, 16–23. [CrossRef] [PubMed]
139. Qu, Y.; Li, H.; Tian, W.; Wang, X.; Wang, X.; Jia, X.; Shi, B.; Song, G.; Tang, Y. Leaching of valuable metals from red mud via batch and continuous processes by using fungi. *Miner. Eng.* **2015**, *81*, 1–4. [CrossRef]
140. Pasechnik, L.A.; Skachkov, V.M.; Chufarov, A.Y.; Suntsov, A.Y.; Yatsenko, S.P. High purity scandium extraction from red mud by novel simple technology. *Hydrometallurgy* **2021**, *202*, 105597. [CrossRef]
141. Khanna, R.; Ellamparuthy, G.; Cayumil, R.; Mishra, S.K.; Mukherjee, P.S. Concentration of Rare Earth Elements during High Temperature Pyrolysis of Waste Printed Circuit Boards. *Waste Manag.* **2018**, *78*, 602–610. [CrossRef]
142. Li, S.; Pan, J.; Zhu, D.; Guo, Z.; Shi, Y.; Dong, T.; Lu, S.; Tian, H. A new route for separation and recovery of Fe, Al and Ti from red mud. *Resour. Conserv. Recycl.* **2021**, *168*, 105314. [CrossRef]
143. Chun, T.; Li, D.; Di, Z.; Long, H.; Tang, L.; Li, F.; Li, Y. Recovery of iron from red mud by high temperature reduction of carbon bearing briquettes. *J. South. Afr. Inst. Min. Metall.* **2017**, *117*, 361–364. [CrossRef]
144. Zhang, Y.; Gao, Q.; Zhao, J.; Li, M.; Qi, Y. Semi-smelting reduction and magnetic separation for the recovery of iron and alumina slag from iron rich bauxite. *Minerals* **2019**, *9*, 223. [CrossRef]
145. Guo, T.; Gao, J.; Xu, H.; Zhao, K.; Shi, X. Nuggets production by direct reduction of high iron red mud. *J. Iron Steel Res. Int.* **2013**, *20*, 24–27. [CrossRef]
146. Samouhos, M.; Taxiarchou, M.; Pilatos, G.; Tsakiridis, P.E.; Devlin, E.; Pissa, M. Controlled reduction of red mud by H$_2$ followed by magnetic separation. *Miner. Eng.* **2017**, *105*, 36–43. [CrossRef]
147. Cardenia, C.; Balomenos, E.; Wai, P.; Tam, Y.; Panias, D. A Combined Soda Sintering and Microwave Reductive Roasting Process of Bauxite Residue for Iron Recovery. *Minerals* **2021**, *11*, 222. [CrossRef]

148. Mombelli, D.; Mapelli, C.; Barella, S.; Gruttadauria, A.; Ragona, M.; Pisu, M.; Viola, A. Characterization of cast iron and slag produced by red muds reduction via Arc Transferred Plasma (ATP) reactor under different smelting conditions. *J. Environ. Chem. Eng.* **2020**, *8*, 104293. [CrossRef]

149. Maihatchi, A.A.; Pons, M.N.; Ricoux, Q.; Goettmann, F.; Lapicque, F. Production of electrolytic iron from red mud in alkaline media. *J. Environ. Manage.* **2020**, *266*, 110547. [CrossRef] [PubMed]

150. Grudinsky, P.; Zinoveev, D.; Pankratov, D.; Semenov, A.; Panova, M.; Kondratiev, A.; Zakunov, A.; Dyubanov, V.; Petelin, A. Influence of Sodium Sulfate Addition on Iron Grain Growth during Carbothermic Roasting of Red Mud Samples with Different Basicity. *Metals* **2020**, *10*, 1571. [CrossRef]

151. Cheng, C.Y.; Misra, V.N.; Clough, J.; Mun, R. Dephosphorization of Western Australian iron ore by hydrometallurgical process. *Miner. Eng.* **1999**, *12*, 1083–1092. [CrossRef]

152. Srivastava, M.P.; Pan, S.K.; Prasad, N.; Mishra, B.K. Characterization and processing of iron ore fines of Kiruburu deposit of India. *Int. J. Miner. Process.* **2001**, *61*, 93–107. [CrossRef]

153. Guider, J.W. Iron ore beneficiation—key to modern steelmaking. *Min. Eng.* **1981**, *33*, 410–413.

154. Dobbins, M.S.; Burnet, G. Production of an iron ore concentrate from the iron-rich fraction of power plant fly ash. *Resour. Conserv. Recycl.* **1982**, *9*, 231–242. [CrossRef]

155. Worldsteel Association. Available online: https://www.worldsteel.org/media-centre/press-releases/2021/Global-crude-steel-output-decreases-by-0.9--in-2020.html (accessed on 2 December 2021).

156. Zhang, Z.L.; Li, Q.; Zou, Z.S. Reduction properties of high alumina iron ore cold bonded pellet with CO–H_2 mixtures. *Ironmak. Steelmak.* **2014**, *41*, 561–567. [CrossRef]

157. Rath, S.; Sahoo, H.; Dhawan, N.; Rao, D.S.; Das, B.; Mishra, B.K. Optimal Recovery of Iron Values from a Low Grade Iron Ore using Reduction Roasting and Magnetic Separation. *Sep. Sci. Technol.* **2014**, *49*, 1927–1936. [CrossRef]

158. Dhunna, R.; Khanna, R.; Mansuri, I.; Sahajwalla, V. Recycling Waste Bakelite as an Alternative Carbon Resource for Ironmaking Applications. *ISIJ* **2014**, *54*, 613–619. [CrossRef]

159. Kongkarat, S.; Khanna, R.; Koshy, P.; O'kane, P.; Sahajwalla, V. Recycling waste polymers in EAF steelmaking: Influence of polymer composition on carbon/slag interactions. *ISIJ* **2012**, *52*, 385–393. [CrossRef]